Regulation of Blood-Brain Barrier Endothelial Cells by Nitric Oxide

Damir Janigro, G. Alexander West, Thien-Son Nguyen, H. Richard Winn

Abstract Nitric oxide (NO) synthesized by vascular endothelial cells is a potent vasodilator substance. The actions of NO extend well beyond its vasodilatory properties, and increasingly, NO has been recognized as an important signal for intercellular and intracellular communication. Recently, NO has been implicated in the regulation of vascular and blood-brain barrier permeability. NO has also been shown to modulate ion channels in excitable cells, thus affecting neuronal firing. We report the results of patch-clamp experiments that show a modulatory action of NO as well as cGMP and cAMP on a hyperpolarization-activated current (I_{ha}) carried by both Na^+ and K^+ ions in blood-brain barrier endothelial cells. I_{ha} was recorded in cells dialyzed with 0.2 mmol/L GTP-γ-S to inhibit a large inwardly rectifying potassium current. This ionic current and its modulation by NO may play a role in the regulation of the transport of ions, nutrients, and other molecules to the brain and serve as an integral part of the blood-brain barrier. The modulation of I_{ha} by a cyclic guanosine nucleotide may also explain previous reports suggesting a role for NO in the regulation of blood-brain barrier function. (*Circ Res.* **1994;75:528-538.**)

Key Words • ion homeostasis • membrane permeability • cyclic nucleotides • hyperpolarization

A precisely regulated extracellular ionic environment in the mammalian central nervous system is vital for normal neuronal function. Capillary and arteriolar endothelial cells (ECs) control the movements of ions and water between blood and brain interstitial fluids; in particular, they regulate the movement of Na^+ and K^+ across the blood-brain barrier,[1,2] preventing excessive potassium accumulation in the cerebrospinal fluid (CSF) and maintaining Na^+ concentrations sufficiently high for action potential generation. A Na^+,K^+-ATPase localized on the abluminal side of brain capillaries[3,4] and an amiloride-sensitive cation channel,[5] acting synergistically with the Na^+-Cl^- transporter,[6] provide a direct path for transendothelial Na^+ transport. Potassium transport is primarily directed from the CSF to the blood so that the blood-brain barrier must play a critical role in brain potassium homeostasis.[1,4,7] Despite the importance of blood-brain barrier function, little is known of the regulation of these ionic fluxes or their modulation by hormones or transmitters.

Endothelium-derived relaxing factor (EDRF) has been identified as nitric oxide (NO) synthesized from the guanidino group of L-arginine.[8,9] The continuous release of NO by the endothelium and the resulting activation of the guanylate cyclase signaling cascade have been shown to impact on the permeability of ECs to solutes and larger molecules.[10-13] In addition, cGMP caused a decrease in the electrical resistance of in vitro blood-brain barrier endothelial monolayers.[14]

The main voltage-dependent ionic current expressed in ECs belongs to the family of inwardly rectifying potassium currents[15-17]; thus, ECs are considered to be electrically "silent" inasmuch as they lack action potential–generating properties. However, membrane oscillations transmitted from neighboring smooth muscle cells have been described, suggesting that in situ ECs may generate action potential–like activity after blockade of smooth muscle potassium channels.[18] It therefore appears that ionic mechanisms other than the inward rectifier can be present in ECs; these ion channels may be normally expressed but require special experimental manipulations to be recorded in isolation (for example, see Reference 19).

We have used the whole-cell variation of the patch-clamp technique[20] to further investigate the expression and possible role of transmembrane ion currents and their modulation by NO in underlying the membrane properties of brain ECs.

Materials and Methods

Cell Culture

Cerebral hemispheres were isolated from male Sprague-Dawley rats (3 to 4 weeks old) as previously described.[19,21] An initial homogenization step and filtration through a 149-μm mesh removed most of the large vessels. The smaller vessels were further dissociated from brain tissue by protease treatment and isolated by centrifugation through dextran. The basement membranes of the vessels were dissociated using collagenase/dispase, and small clusters of rat cerebrovascular ECs were isolated by density gradient centrifugation in Percoll. Clusters of ECs were collected on a 10-μm mesh and plated on poly-D-lysine–coated dishes to remove nonendothelial cells. Nonadherent rat cerebral microvascular EC clusters were then transferred to fibronectin-coated dishes and maintained in DMEM containing 15% equine plasma–derived serum, 4% fetal bovine serum, 50 μg/mL heparin, 100 μg/mL EC growth supplement, 1 mmol/L pyruvate, 2 mmol/L glutamine, nonessential amino acids, vitamins, 100 U/mL penicillin, 100 μg/mL streptomycin, and 0.25 μg/mL Fungizone. These cells were identified as ECs on the basis of positive immunoreactivity for factor VIII antigen and specific uptake of

Received January 4, 1994; accepted May 20, 1994.

From the Department of Neurological Surgery, University of Washington, Harborview Medical Center, Seattle, Wash.

Reprint requests to Damir Janigro, Department of Neurological Surgery, University of Washington, Harborview Medical Center ZX-18, Seattle, WA 98104.

© 1994 American Heart Association, Inc.

Downloaded from http://ahajournals.org by on February 24, 2022

1,1-diocta-decyl-3,3,3′,3′-tetramethyl-indocarbo-cyanine (Dil-Ac-LDL, see Reference 21). These microvascular ECs exhibit morphological characteristics identical to arteriolar and capillary ECs in vivo.

Electrophysiology

Patch-clamp[20] experiments were performed as previously described.[19] Cultured cells (1 to 7 days after plating) were placed in a Petri dish on the modified stage of a Nikon microscope and were continuously perfused with medium containing (mmol/L) NaCl 140, KCl 15, $MgCl_2$ 2, $CaCl_2$ 2, HEPES-OH 10, and dextrose 10 (pH 7.4 with NaOH; temperature, 20°C to 22°C). The intracellular solution used for whole-cell recordings consisted of (mmol/L) KCl 135, $MgCl_2$ 1, $CaCl_2$ 1, EGTA-KOH 10, HEPES-KOH 5, Na_2ATP 5, and Na_2GTP 0.5 (pH 7.3 with KOH; free $[Ca^{2+}]_i$=10 nmol/L). GTP was substituted with guanosine 5′-O-(3′-thiotriphosphate) (GTP-γ-S) as specified in the text. cAMP (sodium salt, Sigma) was added to the pipette solution as indicated in the text. 3-Morpholino-sydnonimine-hydrochloride (SIN1) was obtained from Casella AG. Pertussis toxin (Ptx, from *Bordetella pertussis*, Sigma) was initially dissolved in 50% glycerol containing 50 mmol/L sodium phosphate and 0.5 mol/L NaCl, pH 7.2, at a concentration of 50 μg/mL. Incubation with Ptx (final concentration, 2 μg/mL) was performed for 12 to 20 hours under cell culture conditions. In ion substitution experiments, NaCl was substituted with equimolar *N*-methyl-D-glucamine (Sigma), and the solution was buffered to pH 7.4 with 10 mmol/L HEPES-tetraethylammonium chloride (HEPES-TEA-Cl, Sigma). 8-Bromoadenosine 3′:5′-cyclic monophosphate (8-Br-cAMP) and 8-bromoguanosine 3′:5′-cyclic monophosphate (8-Br-cGMP) (Sigma) were dissolved in the media immediately before the experiments. Solutions were exchanged through a small-diameter rigid plastic tubing (flow rate, 2 mL/min) positioned close (100 μm) to the cell. Recordings were performed with an Axopatch-1C amplifier or with an Axopatch 200A; signals were filtered at 2 kHz. Voltage steps were delivered via a Labmaster-TL1 board driven by PCLAMP software (Axon Instruments, versions 5.5.1 and 6.0). The acquired data were stored on a 486 PC hard disk for off-line analysis. Data were simultaneously digitized at 48 kHz by a DAT A/D converter (BioLogic) and stored in digital format on high-capacity tapes. ECs used in the present study had a resting potential of 60.01±8.5 mV (as measured in current-clamp experiments, $[K]_o$=5 mmol/L, GTP-γ-S=0; n=21). In both voltage- and current-clamp experiments junction potentials were compensated before whole-cell recording. After establishing the whole-cell configuration, they were estimated to be ≈−8.8 mV in 5 $[K]_o$, 140 $[Na]_i$ solutions (by J.P.Calc. Software). This component was not compensated for in figure preparation or data analysis. Electrode resistance was 2 to 3.5 MΩ. Series resistance was not compensated: for a voltage jump of ≈−100 mV and a resulting current of ≈−2 nA (as in Fig 7A and 7D), the estimated voltage error was <10 mV. Total whole-cell current size was quite variable and ranged from a few hundred to several thousand picoamperes, depending on the amount of "cell-contact leak" current due to the monolayer nature of our cell culture preparation (see Reference 22).

Reversal potentials for the hyperpolarization-activated current (I_{ha}) were obtained according to Reference 23. I_{ha} was activated with 1.5- to 3-second hyperpolarization pulses, and the voltage command was then stepped to increasingly depolarizing potentials. The current-voltage data so obtained were linearly fitted (ORIGIN, MicroCal Software, version 3.0 or by PCLAMP), and the intercept (current reversal potential $[E_{ha}]$) was determined. I_{ha} reversal potentials were used to estimate the relative permeability to sodium and potassium according to

$$E_{ha}=RT/F\ \ln_e\{([K]_o+P_{Na/K}[Na]_o)/([K]_i+P_{Na/K}[Na]_i)\}$$

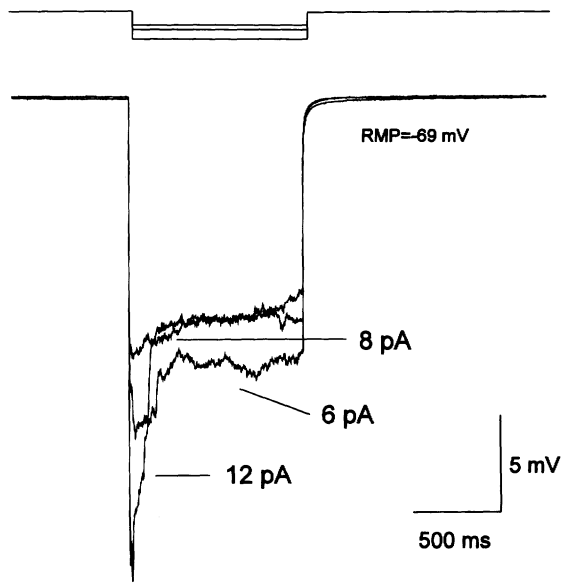

FIG 1. Current-clamp analysis of endothelial cell membrane properties. The cell was maintained at its resting membrane potential (RMP), and square hyperpolarizing current steps were applied at variable (>5-second) intervals. The amount of current injected is shown next to the actual voltage recordings. Note the large depolarizing "sag" following the onset of the current step. This nonlinear membrane voltage behavior increased with increased amounts of injected current. The upper tracing shows the current injection protocol used.

where $P_{Na/K}$ represents the ratio of the permeability to sodium and potassium.

Data points used to construct I_{ha} activation curves are expressed as mean±SEM. Statistical analysis was performed by using Student's *t* test. All the comparisons were made within a single cell exposed to control and NO donor–containing media, as indicated in the figures. Statistical comparisons were made by comparing the extrapolated values for I/I_{max}; asterisks in the figures refer to data points found to be significantly different from the control values.

Results

Whole-cell recordings were performed from 148 cultured ECs. In a preliminary set of experiments we investigated EC membrane responses in current-clamp experiments (Fig 1). Injection of brief negative current steps revealed a pronounced anomalous rectification in rat brain microvascular ECs (RBMECs). To investigate the properties of the anomalous rectification we used the voltage-clamp variation of the whole-cell technique. Hyperpolarizing voltage-clamp steps from a holding potential of −40 mV elicited inward currents displaying pronounced time-dependent inactivation (Fig 2A1), a prominent feature of endothelial inwardly rectifying K^+ currents (I_{IR}).[15-17]

When the nonhydrolyzable GTP analogue GTP-γ-S (0.2 mmol/L, n=40) was added to the recording pipette, the total whole-cell current size as well as the time-dependent inactivation of the I_{IR} was greatly reduced, unmasking another underlying I_{ha} (compare Fig 2A1 and 2A2). Abolishment of I_{IR} by GTP-γ-S has been previously reported in human dermal fibroblasts, guinea pig chromaffin cells, and porcine cerebral ECs.[16,22,24] A typical current-voltage relation for the total whole-cell current as measured after washout of I_{IR} is shown in Fig

Downloaded from http://ahajournals.org by on February 24, 2022

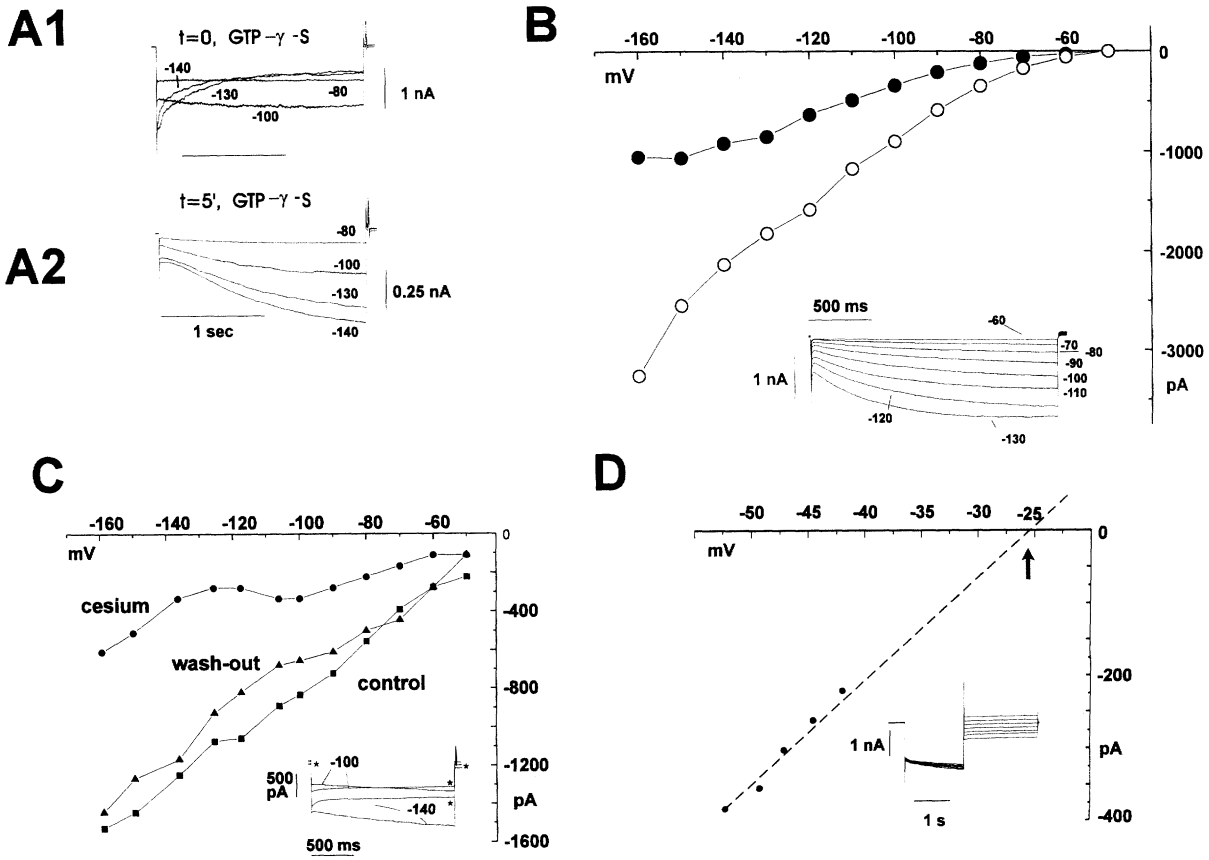

FIG 2. Blockade of inward rectifying potassium currents and characterization of the hyperpolarization-activated current (I_{ha}) in blood-brain-barrier endothelial cells. A1, Inward currents characterized by a time-dependent decay were elicited by negative pulse potentials from a holding potential of −40 mV; 0.2 mmol/L GTP-γ-S was added to pipette solution. The tracings shown refer to whole-cell currents recorded immediately after breaking the seal (t=0). After voltage return to −40 mV the membrane was depolarized to −15 mV for 50 milliseconds to cause inactivation of the time-dependent inward current I_{ha}. A2, Time-dependent inactivating inwardly rectifying potassium current I_{IR} was abolished by intracellular dialysis with GTP-γ-S (t=5 minutes). A hyperpolarization- and time-activated inward current, I_{ha}, was observed at all test potentials. Note the different current scale bars in panels A1 and A2. B, Current-voltage relation obtained in a cell after intracellular loading with GTP-γ-S for 10 minutes. The actual current tracings are shown in the inset; the numbers indicate the amplitude of the test potential (holding potential, −40 mV; pulse duration, 3.5 seconds). The instantaneous current was measured 25 milliseconds after the beginning of the voltage step and was clearly distinguishable from the capacitive transient. C, Reversible block of I_{ha} by 5 mmol/L CsCl (tracings indicated by asterisks) in the presence of GTP-γ-S. Current values refer to steady state: note the shift in holding current after cesium application. D, Extrapolated reversal potential of I_{ha} (arrow). I_{ha} was activated by a voltage step to −140 mV (from −40 mV), and the voltage was then displaced to various potentials for 300 milliseconds.

2B. In Fig 2B filled symbols represent the current recorded at the beginning of the voltage step, whereas open symbols reflect the steady-state current; I_{ha} magnitude is thus represented by the difference between open and closed symbols. Note that I_{ha} activation started at ≈−70 mV. In 20% of the cells, no evident I_{IR} component was recorded, and the predominant current activated by hyperpolarization was I_{ha}, thus suggesting that GTP-γ-S was not a prerequisite to record I_{ha}. Data obtained from these cells were not used for data analysis, nor were these cells used for the pharmacological experiments described below. I_{ha} was sensitive to blockade by extracellular Cs^+ (2 to 5 mmol/L, Fig 2C; the inset shows the actual current tracing at the test potentials indicated). E_{ha} was derived according to Maccaferri et al[23] and was estimated to be ≈−25 mV (in 140 mmol/L $[Na^+]_o$ and 15 mmol/L $[K^+]_o$, Fig 2D). In addition, E_{ha} depended on extracellular $[Na^+]_o$ and $[K^+]_o$, consistent with a current carried by sodium and potassium.[23,25,26] Cesium sensitivity and hyperpolarization- and time-dependent activation are characteristics of the so-called "pacemaker" current involved in the autorhythmic potential generation in the heart[25,26,27] and the regulation of the firing properties of central nervous system neurons.[23,28-31]

In an attempt to further characterize the properties of the effects of GTP-γ-S on the inwardly rectifying component, we studied the behavior of the instantaneous current elicited by applying hyperpolarizing steps during intracellular dialysis with GTP-γ-S (Fig 3).The protocol used is described in Fig 3A: cells were voltage clamped at −40 mV, and hyperpolarizing steps to −140 mV were applied at 30-second intervals. The instantaneous current component (open asterisk in Fig 3A; the open circle refers to the current recorded after 10 minutes of dialysis with GTP-γ-S) was then plotted against time elapsed after establishing the whole-cell configuration (Fig 3B through 3D). When GTP-γ-S was present in the recording pipette, the instantaneous current component decreased over time (Fig 3B, n=12; data are expressed as mean±SEM). When recordings were performed with pipettes containing 0.5 mmol/L

Downloaded from http://ahajournals.org by on February 24, 2022

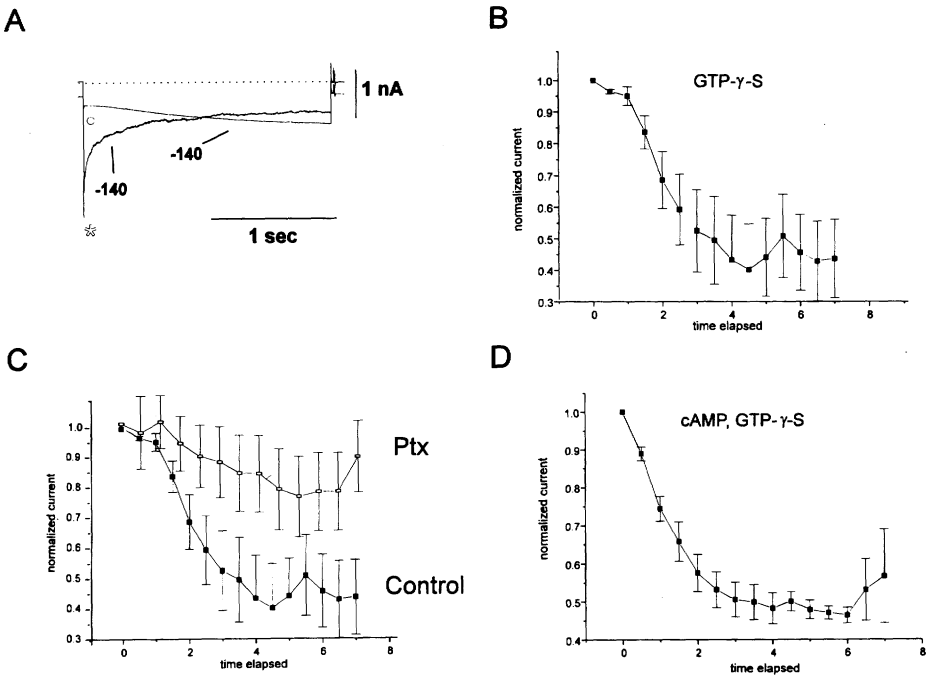

FIG 3. Effects of intracellular dialysis on inward currents during whole-cell recordings. A, Protocol used to activate inward currents is shown. From a holding potential of −40 mV the cell membrane was clamped to −140 mV to evoke inward currents at variable intervals. The current tracing marked with an open circle refers to the same recording protocol, but it was performed after dialysis with GTP-γ-S for 10 minutes; the other current tracing was recorded immediately after rupturing the patch and establishing the whole-cell configuration. The instantaneous current jump was measured at the time indicated by the asterisk. The dashed tracing represents 0 nA. B, Graph shows that recording with pipettes containing GTP-γ-S caused a progressive decrease of the instantaneous inward current (n=12). C, Graph shows that the decrease shown in panel B was almost entirely prevented by pretreatment of the cells with pertussis toxin (Ptx) (n=6). D, Graph shows that when the recordings were performed with pipettes containing both GTP-γ-S and cAMP (0.2 mmol/L, disodium salt), a time-dependent washout of inwardly rectifying potassium current identical to that obtained with GTP-γ-S alone was observed (n=4). Data are expressed as mean±SEM of normalized currents.

guanosine 5′-3′-triphosphate (disodium salt), no significant run-down of inward currents was observed during the first 10 minutes of recording (data not shown). In order to investigate the possible involvement of inhibitory G proteins, we pretreated the cells with Ptx (see Reference 32). Fig 3C shows the results of an experiment identical to that described in Fig 3B, but the results are compared with data obtained from six cells previously exposed to 2 mg/mL Ptx for 16 hours. Note that pretreatment with Ptx caused a significant reduction of the effects of GTP-γ-S (n=6 for both control and Ptx-treated cells; $P<.005$ at t=7 minutes). We also investigated the possible involvement of cyclic nucleotides in the mechanism underlying I_{IR} washout (Fig 3D). Simultaneous exposure of the cells to GTP-γ-S and cAMP (0.2 mmol/L) did not cause any significant effect on the run-down of I_{IR} (n=4).

The ionic nature of I_{ha} was further investigated in ion substitution experiments after prolonged recordings with pipettes containing GTP-γ-S (Fig 4). Voltage protocols similar to those described above were used to evoke inward currents during hyperpolarizing steps. Cells were kept at a holding potential of −40 mV, and voltage steps of varying amplitudes were delivered. Partial removal of extracellular sodium (to 50%, substituted with equimolar *N*-methyl-D-glucamine) caused a decrease of the inward current (Fig 4A and 4B). These data are summarized in Fig 4C in a plot of the current-voltage relation for the currents shown in panels A and B. Note that partial sodium removal caused a negative shift of E_{ha}, as expected for a current partially carried by sodium. The shift in current reversal potential following manipulations of the external sodium concentrations was not accompanied by changes in current slope conductance. Total replacement of sodium with equimolar *N*-methyl-D-glucamine caused an almost total abolishment of I_{ha} (Fig 4D). Fig 4D1 shows the currents recorded under control ionic conditions (140 mmol/L $[NaCl]_o$). Note that the time-dependent activation of the inward current was followed by a slow current decay; this behavior was frequently observed and is attributable to residual I_{IR} channels. In fact, intracellular dialysis with GTP-γ-S caused only a 50% decrease in inward currents even after long whole-cell recordings (see Fig 2B). Removal of extracellular sodium (by substitution with *N*-methyl-D-glucamine) caused a virtual disappearance of I_{ha}, leaving the instantaneous current (I_{IR}) unchanged (Fig 4D2).

The dependency of I_{ha} to changes in extracellular potassium concentrations was similarly investigated in 15 cells (Fig 5). Simultaneous manipulations of extracellular K^+ (from 15 to 48 mmol/L) and Na^+ (from 140 to 97 mmol/L) caused a dramatic increase in I_{ha} (Fig 5A1 and 5A2) and a positive shift in E_{ha} (Fig 5B). Thus, whereas replacement of extracellular sodium with *N*-methyl-D-glucamine caused a decrease in current size (see Fig 4), replacement with equimolar KCl caused a current increase, suggesting an involvement of potassium ions in

Downloaded from http://ahajournals.org by on February 24, 2022

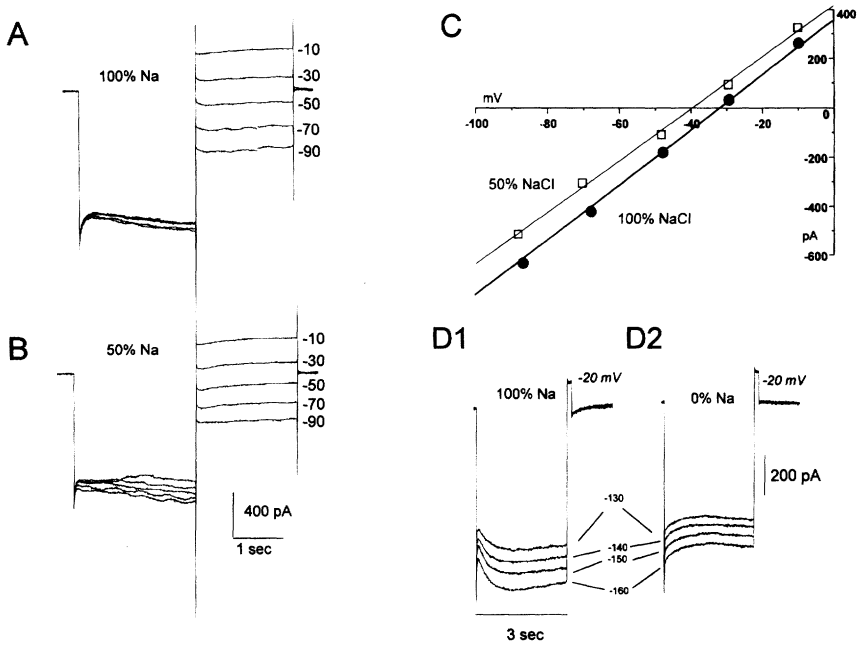

FIG 4. Ionic substitution experiments used to determine the ionic nature of hyperpolarization-activated current I_{ha}. A and B, Tracings showing that partial removal of extracellular sodium, substituted with equimolar *N*-methyl-D-glucamine, caused a decrease of the inward current activated by cell hyperpolarization. The voltage was then stepped to the potentials indicated and the currents evoked were measured in respect to the holding current. All tracings were digitally leak subtracted. The solution contained 10 mmol/L tetraethylammonium chloride (TEA-Cl) to block outward currents, and the cells were dialyzed with GTP-γ-S. C, Current-voltage plot of the traces shown in panels A and B. Data points were fitted by a least-squares fitting protocol. Note that partial sodium removal caused a negative shift in I_{ha} reversal potential. D1, Tracings showing I_{ha} evoked from a potential of −40 mV in a solution containing 140 mmol/L NaCl. D2, Tracings showing that when the extracellular medium was changed to one containing no sodium, the inward current displaying time-dependent activation was greatly reduced. The extracellular solutions were both buffered with 10 mmol/L HEPES–TEA-Cl (see "Materials and Methods"). A voltage step to −20 mV was applied upon return to holding potential to cause inactivation of the inward current.

channel conductance (see also References 23 and 33). In fact, in addition to a shift in E_{ha}, high-potassium solutions caused a dramatic increase in slope conductance (Fig 5C), from 8.06±3.1 to 20.01±1.6 nanosiemens in 15 and 48 mmol/L $[K]_o$, respectively (n=12). The increase in conductance was entirely due to extracellular potassium since similar manipulations of external sodium did not show any appreciable effect of $[Na]_o$ on I_{ha} slope conductance. The permeability ratio for Na^+ and K^+ ions was determined from experiments performed in different extracellular sodium and potassium concentrations. The results obtained from cells bathed in 15 mmol/L potassium and 140 mmol/L sodium gave a $P_{Na/K}$ value of 0.09, suggesting that in RBMECs kept under quasi-physiological ionic gradients, I_{ha} is significantly more permeant to K^+ than Na^+ ions.

The role of endogenous NO in the regulation of a variety of physiological processes is clearly established.[8-13] Recent evidence has suggested that NO may also influence the electrophysiological characteristics of neuronal and vascular smooth muscle cells.[31,34] In addition, modulation of the cardiac pacemaker current (I_f) by intracellular messengers such as cAMP or cGMP has been reported.[35] We have therefore investigated the effects of exposing blood-brain barrier ECs to NO, cGMP, and cAMP (Figs 6 through 8). Exposure of the cells to NO was first achieved by applying an NO-generating substance (sodium nitroprusside [SNP]) to the cells (Fig 6 and Reference 36). Experiments in which the effects of SNP were investigated were usually performed with pipettes containing 0.5 mmol/L Na_2GTP in addition to GTP-γ-S (0.2 mmol/L). High concentrations of SNP (1 mmol/L) caused an increase of I_{ha} evoked by hyperpolarizing steps (n=10, Fig 5A) in the presence of 0.5 mmol/L $[GTP]_i$. This effect was observed in the whole range of voltages tested (Fig 6B). When hydrolyzable GTP was not present in the recording pipette, SNP failed to exert any effects on I_{ha} (n=5). NO donors caused a downward shift of the holding current, possibly due to the activation of I_{ha} channels activated at the holding potential. A negative shift in holding current is in fact consistent with the activation of a depolarizing ion influx. The concentration of SNP used in our experiments (1 mmol/L) caused a maximal (87% of control) vasodilation of rat pial arterioles in vivo and in vitro (data not shown). In two cells a transient current decrease was observed before current increase during perfusion with SNP; in one cell SNP application was ineffective. In two different cells the instantaneous component was also increased by exposure to the NO-releasing substance. The overall (n=6) increase in inward current observed after exposure to SNP was due to a 19.1±3.01-mV shift of the I_{ha} activation curve (Fig 6C). Current activation was measured by normalizing tail currents evoked by return to the holding potential following hyperpolarizing voltage steps with respect to maximal current amplitude before (filled symbols) and after (open circles) exposure to SNP. In Fig 6C these values are plotted against the value of the preceding membrane potentials; the inset shows the actual tail current tracings from −120 to −40 mV. Since the physiological actions of NO are normally achieved at significantly lower concentrations of NO donor molecules, we performed additional experiments where micromolar concentrations of the NO donor molecule were applied to the cells (Fig 7). Applications of 1 to 10

Downloaded from http://ahajournals.org by on February 24, 2022

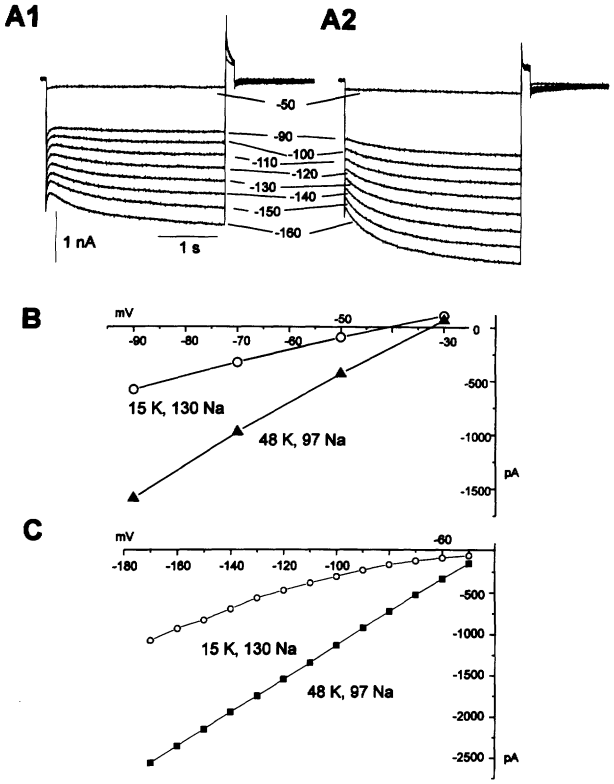

FIG 5. Hyperpolarization-activated current (I_{ha}) is carried by both sodium and potassium. Whole-cell inward currents were evoked from a holding potential of −40 mV in 15 mmol/L $[K]_o$ and 140 mmol/L $[Na]_i$ (A1) and 48 mmol/L $[K]_o$ and 97 mmol/L $[Na]_o$ (A2) external solutions. The test potentials are indicated by the numbers next to the tracings. Note the increase in I_{ha} after increasing extracellular potassium and decreasing sodium. B shows values of current reversal potential (E_{ha}) in different concentrations of external cations. Current values used to extrapolate E_{ha} were obtained as described in Figs 2 and 4; the data points were fitted with a straight line by a PCLAMP fitting routine. C, Current-voltage plot of the fully activated currents shown in panels A1 and A2. Note the conductance increase caused by increasing $[K]_o$.

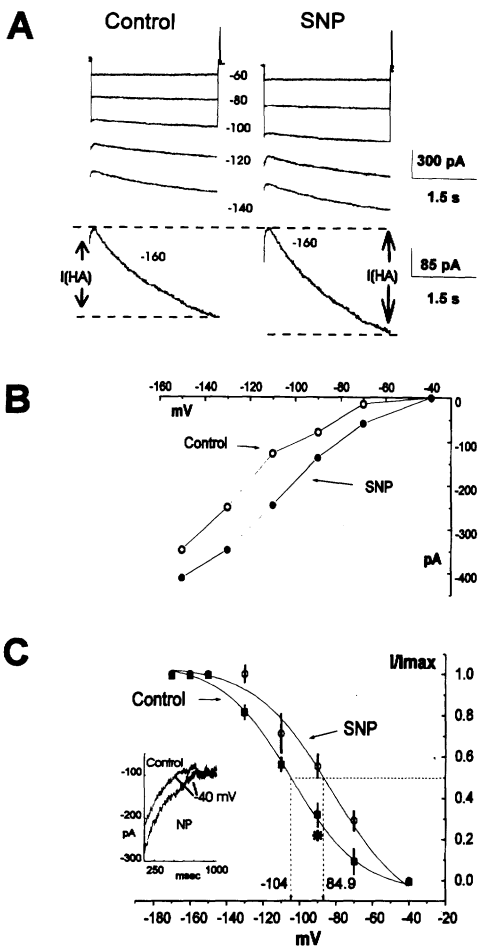

FIG 6. Effects of sodium nitroprusside (SNP) on hyperpolarization-activated current [I_{ha}]. A, SNP increased I_{ha} at all test potentials. The time-dependent inward current was measured as the difference between the instantaneous current jump immediately following the voltage step and the current recorded at the end of the pulse as indicated by the arrows. The test voltages applied are indicated by the numbers next to the current tracings. The tracings recorded at −160 mV are expanded to emphasize the current increase observed after SNP. B, Current-voltage relation of the currents recorded in panel A is shown. Data points were obtained as described in panel A. C, SNP caused a positive shift of the activation curve. Mean±SEM of normalized tail currents are plotted against membrane potential. The difference between control and SNP-treated cells was significant at $P<.002$ (at $I/I_{max}=0.5$, asterisk). A sample of the tail currents (from a test pulse of −120 mV) used to extrapolate the data shown in panel C is depicted in the inset. Current tracings refer to tail current recorded on return to −40 mV after a test pulse of −120 mV; the last portions of the tracings were digitized at a higher sampling rate.

μmol/L SNP caused a dose-dependent increase in I_{ha} attributable to a shift in the activation curve voltage dependency (Fig 7A and 7C; $[K]_o=48$ mmol/L, $[Na]_o=97$ mmol/L; n=6 for SNP-1 μmol/L, $P<.05$; n=4 for SNP=10 μmol/L, $P<.001$). The apparent threshold for the effect was at 500 nmol/L SNP (Fig 7B and 7D). Lower (10 nmol/L) concentrations of SNP failed to exert any appreciable effect on I_{ha}.

Since SNP has been shown to exert biological actions not related to its potency as NO donor,[36] we challenged the cells with SIN1 (see Reference 31), which releases NO by a mechanism different from SNP (Fig 8). Similar to findings with SNP, 1 μmol/L SIN1 caused an increase in I_{ha} (Fig 8A1 and 8A2). The voltage protocol used in these experiments to elicit I_{ha} differed inasmuch as the cell membrane potential was first stepped to variable-length hyperpolarizing values and then stepped further to −160 mV to fully activate the residual current; membrane potential was finally stepped back to the holding potential value. The activation curve was then constructed by measuring the "tail" currents at −160 mV and by plotting these values against the potentials of the test pulses. Exposure of the cells (n=6) to SIN1 caused an increase of the current paralleled by a shift in current activation curve (Fig 8C, $[K]_o=48$ mmol/L, $[Na]_o=97$ mmol/L; n=6, $P<.001$ at $I/I_{max}=0.5$). In this respect, SIN1 appeared to be more potent than SNP (compare Figs 7 and 8). Similar results were obtained with higher (0.1 mmol/L) concentrations of SIN1 (data not shown). In 3 of 9 cells, in addition to the effects described above, SIN1 exerted a modest effect on the time-independent current component that was due to a reversible decrease of the initial jump of the inward current (Fig 8B). In spite of a decreased instantaneous

Downloaded from http://ahajournals.org by on February 24, 2022

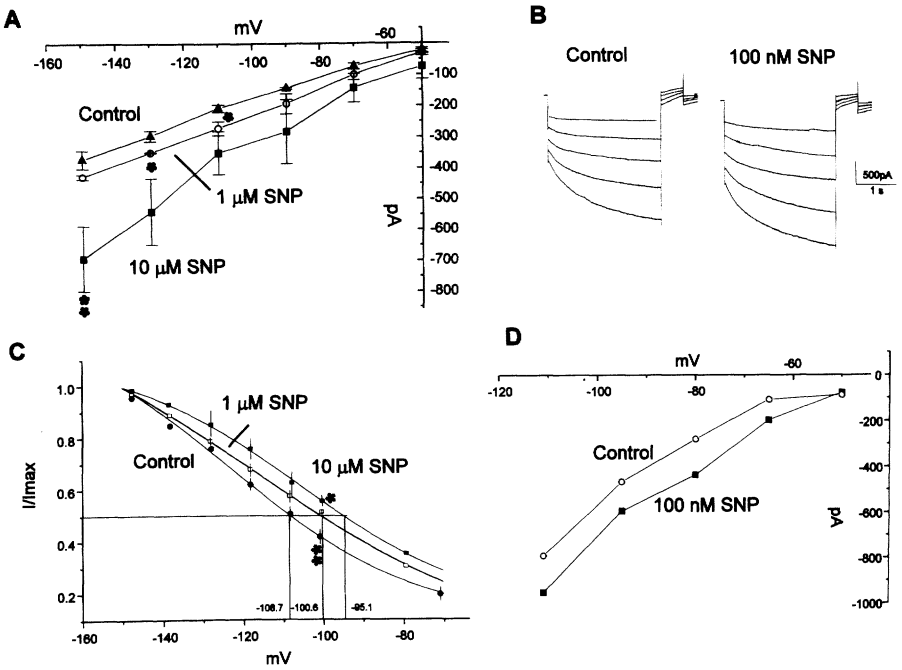

FIG 7. Effects of low concentrations of sodium nitroprusside (SNP) on hyperpolarization-activated current (I_{ha}). A,Current-voltage (I/V) plot summarizing data (expressed as mean±SEM) obtained from four experiments. Values significantly different from control are indicated by an asterisk. The cells were exposed to increasing concentrations of SNP, and I_{ha} was evoked from a holding potential of −40 mV. The apparent threshold for SNP-induced increases in whole-cell currents was at 500 nmol/L (B and D). C, Activation curves obtained from the cells used for the I/V plot shown in panel A. The current increases were due to a positive shift of the activation curve caused by SNP ($[K]_o$=48 mmol/L, $[Na]_o$=97 mmol/L).

current, SIN1 caused an increase of the time-dependent current (Fig 8B, lower panel).

NO is believed to exert its functions by activating a soluble guanylate cyclase, leading to increased intracellular cGMP.[8,9] Modulation of a current system similar to I_{ha} by intracellular cAMP and cGMP in cardiac cells has been described,[35] and recently NO has been shown to increase a hyperpolarization-activated mixed Na^+/K^+ current in thalamic neuronal cells.[31] In blood-brain barrier ECs, the membrane-permeant cGMP analogue 8-Br-cGMP (1 mmol/L) caused an increase in I_{ha} at all potentials (Fig 9A and 9B). This effect was primarily on the time-dependent (or steady-state) current component and not on the instantaneous component (Fig 9B). cGMP caused a 9.01±2.09-mV shift in the voltage dependence of I_{ha} activation (n=6, Fig 9C). Intracellular dialysis with cAMP also increased I_{ha} (Fig 9D), and this effect was likewise due to a positive shift in the activation curve (data not shown). In these experiments, in addition to GTP-γ-S 0.2 mmol/L, cAMP was added to the recording pipette, and the properties of I_{IR} (instantaneous current) and I_{ha} (difference between instantaneous and steady-state currents) were monitored over time. Similar results, ie, a shift of I_{ha} activation proper-

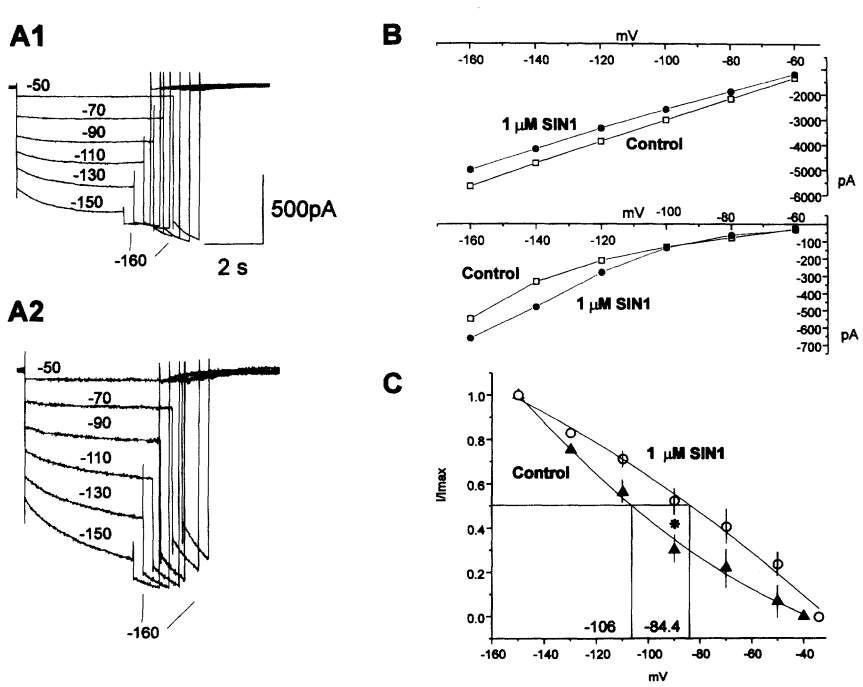

FIG 8. 3-Morpholino-sydnonimine-hydrochloride (SIN1, 1 μmol/L) causes activation of hyperpolarization-activated current (I_{ha}). A1, Cells were held at −40 mV, and the potential was then stepped to negative values to activate I_{ha}. Further activation of I_{ha} was achieved by stepping the membrane potential to −160 mV before return to holding potential. Note that current activation becomes faster with larger hyperpolarizations. A2, After perfusion of the cell with SIN1 for over 2 minutes, the time-dependent current component grew in size and caused an increased rate of I_{ha} activation. B, Current-voltage plot of the current recorded from three cells exposed to SIN1 is shown. In addition to an increase in the time-dependent current (lower panel, the current was measured as difference of the instantaneous jump from steady-state), SIN1 caused a decrease of the time-independent current component (upper panel, measured at the beginning of the voltage step). C, The action of SIN1 on I_{HA} is due to a shift of the current activation curve. Data are presented as mean±SEM (n=6; $[K]_o$=48 mmol/L, $[Na]_o$=97 mmol/L). *P<.001 at I/I_{max}=0.5.

Downloaded from http://ahajournals.org by on February 24, 2022

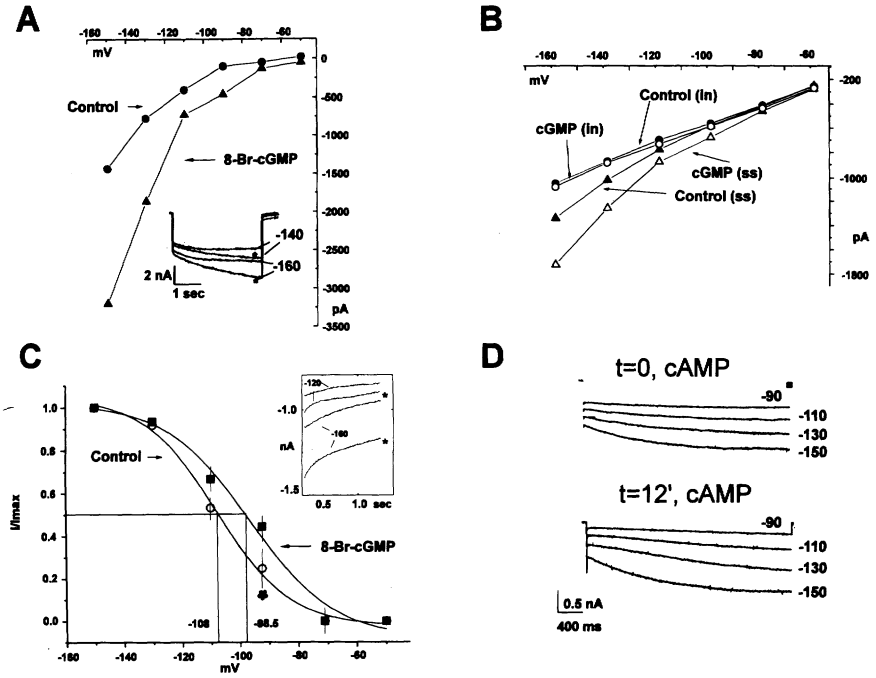

FIG 9. Effect of cGMP and cAMP on the hyperpolarization-activated current (I_{ha}). A, Superfusion with 1 mmol/L 8-bromo-cGMP increased I_{ha} at all test potentials shown in the current-voltage relation. Inset at bottom shows individual current recordings at test potentials −140 and −160 mV. B, Similar to sodium nitroprusside (SNP), cGMP primarily affected the time-dependent current component (steady-state[ss]), leaving the instantaneous (in) jump virtually unchanged. C, 8-Bromo-cGMP caused a positive shift in the activation curve from −105 to −96 mV (*P<.005). Tail currents are shown in the inset; here and in panel A, the asterisk next to the current tracings indicates tracings obtained after 8-bromo-cGMP application. D, Similar to SNP and cGMP, cAMP also increased I_{ha}; intracellular dialysis with cAMP caused an increase of I_{ha}. Holding potential was −40 mV, and the numbers indicate the test potentials.

ties, were seen by manipulation of $[cAMP]_i$ by extracellular application of forskolin (100 μmol/L) or 8-Br-cAMP (1 mmol/L, not shown). The recordings shown in Figs 5 through 9 were taken from cells dialyzed with the nonhydrolyzable GTP analogue GTP-γ-S for more than 10 minutes.

Discussion

Brain ECs constitute the blood-brain barrier and play an important role in the regulation of cerebral blood flow by releasing vasoactive substances, including EDRF, or NO. Voltage-dependent and receptor-activated as well as ATP-sensitive ion channels have been involved in a variety of EC functions, including NO release and ion permeability of the blood-brain barrier.[16,17,19] NO- and cAMP-dependent mechanisms have been implicated in the regulation of EC permeability,[10-14,37] but the mechanisms underlying these actions are still unknown. In the present study we describe a novel ionic mechanism that may play an important role in the regulation of blood-brain barrier permeability, a mixed Na^+-K^+ current that provides an ideal mechanism (in conjunction with the Na^+-K^+ pumping mechanisms, Fig 10) for the maintenance of physiological ionic concentrations in the CSF. In addition, our results demonstrate that I_{ha} is similar to neuronal I_h[23,28-30] and cardiac I_f.[25,26] To our knowledge, this is the first report describing a cesium-sensitive, hyperpolarization-activated cation Na^+-K^+current in nonexcitable cells.

Our first evidence of the presence of an inward current activated by cell hyperpolarization was obtained from current-clamp experiments (Fig 1). However, a detailed analysis of I_{ha} behavior resulted from voltage-clamp experiments. Our current-clamp results are consistent with the voltage-clamp data demonstrating the expression of a current similar to I_f (or I_h) in brain ECs. In fact, the delayed time of onset of the anomalous rectification observed during current injection steps indicates the involvement of an inward current activating over time during membrane hyperpolarization, ie, I_{ha}.

The "unmasking" of I_{ha} was achieved by causing run-down of I_{IR} with GTP-γ-S (Figs 2 and 3). In fact, under physiological conditions (ie, hydrolyzable GTP in the pipette solution) the predominant whole-cell current observed during hyperpolarizing steps from a holding potential of −40 mV was a potassium current displaying marked time-dependent inactivation (Fig 2A). This current has been described in detail[16,17] and belongs to the inwardly rectifying current family. As previously described in a number of cell types, including brain microvascular ECs,[21,24,38] when whole-cell recordings were performed to induce intracellular dialysis with GTP-γ-S, this large potassium current component decreased dramatically over time (see Fig 3); in our experiments on ECs this manipulation led to the unmasking of an underlying inward current, I_{ha}. It may be argued that enhancement of a G protein–dependent process, rather than a blockade of I_{IR}, may have caused the appearance of I_{ha}. This is unlikely since I_{ha} was observed in "naive" cells that were not exposed to GTP-γ-S or GTP (data not shown) and since I_{ha} recorded in these cells had activation properties indistinguishable from those reported in Fig 2. In addition, the results shown in Fig 3A provide direct evidence that the instantaneous current (I_{IR}) was greatly decreased by GTP-γ-S. In addition, intracellular cAMP caused an increase in the time-dependent I_{ha} component while causing little if any effect on I_{IR}.

Interestingly, Hoyer et al[16] did not observe any I_{ha}-like conductance activation after reduction of the endothelial inward rectifier with GTP-γ-S. This appears to be due to the different voltage protocols used in those experiments. In fact, at moderately negative potentials (−90 to −110, ≈I_{ha} half-activation point, see for example Fig 5A) and in low external K^+, I_{ha} activates slowly and long-lasting hyperpolarizing voltage steps are needed to fully activate the current. The data reported

Downloaded from http://ahajournals.org by on February 24, 2022

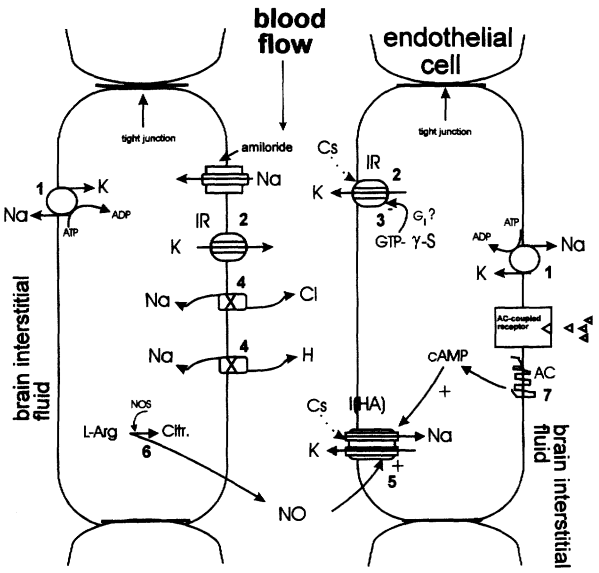

FIG 10. Diagram shows proposed role for hyperpolarization-activated current (I_{ha}) in the regulation of blood-brain barrier permeability. Endothelial cells (ECs) effectively isolate the brain from the blood by allowing little movement of molecules as a result of the presence of tight junctions between ECs and the extremely low resting membrane permeability of ECs. K^+ ions are pumped from the brain into the ECs by an ATP-dependent carrier mechanism exchanging Na^+ and K^+ against their electrochemical gradient (1). Potassium accumulation into ECs is prevented by a voltage-dependent flux into the blood primarily due to the inward rectifying channels (IR, see 2). Results of the present study suggest that modulation by an inhibitory GTP-binding protein (G_i) may be involved in the regulation of potassium homeostasis (3). Sodium uptake from the blood into the brain may be achieved by exchange mechanisms also involved in the maintenance of electroneutrality of the system (ie, extruding Cl^-) and in the regulation of acid-base equilibrium (by excluding protons from the ECs, [4]) or via an amiloride-sensitive ion channel. I_{ha} provides an additional, energy-independent mechanism that allows entry of Na^+ and efflux of K^+ into and from ECs according to their passive electric gradient (5). Nitric oxide (NO), synthesized intracellularly from L-arginine (L-Arg) by endothelial NO-synthase (NOS) enzymes and released into the extracellular space, may act in an autocrine fashion on EC I_{ha} (6), promoting an ion exchange mechanism linking extracellular signaling (ie, receptor activation [7]) to blood-brain barrier function. Citr.=citrulline.

in Reference 16 were obtained by applying short voltage steps primarily designed to elicit the inward rectifier current, which activates almost instantaneously (see Figs 2A and 3A). Thus, I_{ha} can be evoked only when appropriate voltage-clamp protocols are applied to the cells.

The effects of GTP-γ-S were prevented by preincubation of the cells with Ptx, further suggesting the involvement of an inhibitory G protein acting on the inward rectifier.[16,24] It is also worth noting that cAMP, which caused an increase of the I_{ha} current component (see Fig 7D), failed to exert any effect on the time course of I_{IR} washout as judged by measurements of the instantaneous current component, suggesting that activation of I_{ha} by cyclic nucleotides and inhibition of the inward rectifier by G proteins are separate mechanisms. However, our results cannot completely rule out a direct or indirect involvement of GTP-binding proteins in the modulation of I_{ha}.[39] A more definitive answer to the question would have resulted from cell-attached, single-channel experiments to resolve I_{ha} from I_{IR} channel openings, but these have proven extremely difficult to perform in ECs, possibly because of the very low (<1 picosiemen) conductance of I_{ha} channels, as reported for cardiac sinoatrial node cells (see Reference 26).

Another possible explanation of our results with GTP-γ-S may suggest that GTP-γ-S caused a modification of the inward rectifier, resulting in the recordings we attribute to I_{ha}. We believe that this is unlikely and that I_{IR} and I_{ha} are two separate entities. This is due to several reasons, including the following: (1) As we have shown in the present study and as reported by numerous laboratories, h-type currents are carried by both sodium and potassium, while the sodium permeability of I_{IR} is negligible. (2) The kinetics of current time-dependent behavior of I_{IR} is different from that of I_{ha}. In fact, the potassium current displays marked time-dependent inactivation during negative voltage steps, while I_{ha} grows larger with time at the same potentials. (3) The reversal potentials for the two currents are different; this is attributable to their different ionic nature. (4) GTP-γ-S did not exert any effect on I_{ha} and cAMP did not alter I_{IR} washout. Finally, the gene product responsible for the expression of the inward rectifier does not encode ion channels similar to those responsible for I_{ha}.[40]

I_{ha} resembled cardiac I_f and neuronal I_h (or I_q) because of its sensitivity to extracellular cesium and its ionic nature. In addition, current-activation properties and time dependency correlated well with those of hyperpolarization-activated cationic currents. Our results in Figs 4 and 5 provide direct evidence of an inward current activated by hyperpolarization and carried by Na^+ and K^+ ions. The extrapolated reversal potential (E_{ha}, Fig 2D) and its shifts during ionic substitutions were consistent with this hypothesis. Perhaps surprisingly, total replacement of extracellular sodium caused a virtual disappearance of I_{ha}, suggesting that under zero $[Na^+]_o$ conditions the permeability properties of the channels may differ. As previously shown for cardiac I_f, I_{ha} conductance (as derived from the I/V relation slope, not shown) was increased by extracellular potassium (from 5 to 48 mmol/L), suggesting that in addition to being permeant to K^+, the channel is also sensitive to activation by extracellular cations.[33] Under quasi-physiological conditions, the permeability ratio P_{Na}/P_K obtained from our experiments on endothelial I_{ha} suggests that potassium is approximately 10 times more permeant than sodium.

A further similarity between neuronal, cardiac, and endothelial Na^+-K^+ inward currents was found when RBMECs were exposed to NO donor substances or to cGMP (Figs 5 through 7). SNP caused an increase in I_{ha} due to a positive shift of current activation properties. Similarly, SIN1 increased I_{ha}, thus ruling out nonspecific effects (such as release of CN ions by SNP) due to the molecular nature of the NO donor molecule used.[31] In further support of an involvement of NO in the modulation of I_{ha} is the fact that pharmacological manipulations aimed to directly increase the intracellular concentration of cGMP (such as exposure to 8-Br-cGMP) caused a similar effect. In addition, cells internally dialyzed with the nonhydrolyzable GTP analogue GTP-γ-S (and no GTP) failed to respond to the NO donor SNP, again suggesting that the effects of SNP were due to molecular NO release and subsequent activation of

Downloaded from http://ahajournals.org by on February 24, 2022

endothelial guanylate cyclase.[8,9] Both the effects of NO released by NO donor agents and cGMP were specific on I_{ha} and did not cause any appreciable or consistent effect on the residual I_{IR} current component spared by GTP-γ-S delivered through the recording pipette. In addition to cGMP, cAMP and forskolin (or extracellular 8-Br-cAMP) also caused a similar increase in I_{ha}. Identical findings have been reported for I_f, the cardiac counterpart to I_{ha}.[35]

It is often assumed that ECs that constitute the blood-brain barrier consist primarily of the capillary endothelium, while precapillary, arteriolar ECs are believed to be involved in the regulation of vascular tone. Our cell-culturing technique did not allow for a rigorous discrimination between blood-brain barrier and arteriolar ECs.[21] However, a hyperpolarization-activated Na^+-K^+ current in brain ECs may play a role in both blood-brain barrier permeability and control of vascular tone. EC resting potential and its regulation of intracellular calcium seem to be strictly related to the amount of endothelial NO released by the endothelium.[9,15,19] This appears to depend on the calcium sensitivity of the constitutive NO-synthesizing enzyme.[9] Activation of I_{ha} by NO would result in membrane depolarization, thus decreasing the driving force for calcium entry, leading to decreased NO release. This mechanism may, at least in part, explain the NO-induced decrease of NO release reported by Ignarro and coworkers (Buga et al).[41]

We also propose a role for I_{ha} in the regulation of blood-brain barrier permeability (Fig 10). In the suggested model of blood-brain barrier, inclusive of I_{ha}, excess potassium is pumped from the brain into ECs by an energy-dependent Na^+-K^+ pump,[2] located extraluminally; the same system provides a pathway for Na^+ entry into the brain, possibly against its electrochemical gradient.[1,3] The source for endothelial Na^+ (and a pathway for potassium clearance into the bloodstream) is provided by (1) an amiloride-sensitive nonspecific cation pore[5]; (2) an inwardly rectifying potassium channel,[16,17] possibly modulated by an inhibitory G protein; and (3) I_{ha} located on the intraluminal side of the EC membrane. The intracellular modulation of I_{ha} described in the present study thus explains previous findings linking NO, cGMP, and cAMP to vascular permeability.[11,14,42] However, evidence against an involvement of cGMP (or cAMP and SNP) in the regulation of transendothelial resistance has also been reported.[43] These apparently contradictory results were obtained under different experimental conditions (in vitro cultured endothelial cells versus in vivo brain venules) and from different species (rodent versus amphibian). In addition, the experiments supporting a role for cGMP in blood-brain barrier function[17] were performed on tight junction–forming ECs pretreated with astrocyte-derived conditioned media, thus mimicking the physiology of the mammalian blood-brain barrier. Because of the speculative role for the involvement of cyclic nucleotide–regulated ion channels in the physiology of blood-brain barrier transport, additional experimental evidence is required to fully understand how and if I_{ha} may affect transendothelial resistance.

A possible role for I_{ha} in the transendothelial transport of Na^+ and K^+ ions rests on the hypotheses (1) that the Na^+-K^+ pumping mechanisms are segregated on the extraluminal portion of EC membranes; (2) that I_{ha} channels are located intraluminally (see Fig 10); (3) that despite the low (<1 picosiemen) single-channel conductance reported for its cardiac counterpart I_f,[26] I_{ha} channel density is sufficient to cause a significant effect on cell resting membrane potential. While ample experimental evidence supports the first hypothesis,[3,4] the latter could be verified by using selective markers for I_{ha}, but selective probes for I_{ha} are not available. However, ion currents have been recorded from both intraluminal and extraluminal membrane patches,[16,39] providing indirect evidence that I_{ha} channels may be expressed also, if not exclusively, on the intraluminal side of blood-brain barrier ECs. The third hypothesis is confirmed by the data shown in Fig 1, showing that cell membrane hyperpolarization during current clamp is in part prevented by the generation of a depolarizing "sag" attributable to I_{ha} (see also References 23,28,30). Alternatively, the depolarizing potential may be caused by the activation of low-threshold calcium channels. This seems unlikely, however, since these cells do not express voltage-operated calcium channels.[19]

In addition to I_{ha}, other cation-permeant channels have been described in ECs, including an amiloride-sensitive sodium channel[5] and a stretch-activated channel (SAC).[44] The inward current described in this study was sensitive to blockade by cesium but not amiloride (data not shown), thus ruling out a similarity with the channel described by Vigne et al.[5] Moreover, while I_{ha} shares some characteristics in common with the current flowing through stretch-activated channels (ie, permeability to Na^+ and K^+), there are several biophysical properties that make a comparison between the two channels unlikely: (1) SACs are permeant to Ca^+ ions, while I_{ha} is selective for Na^+ and K^+; (2) I_{ha} is blocked, while SACs are permeant to millimolar concentrations of cesium; (3) I_{ha} activates at negative potentials, while SACs are open at $\approx$20 mV; and (4) I_{ha} belongs to the family of voltage-dependent, nucleotide-modulated channels, and thus does not require mechanical stimuli for activation.

Our results suggest that ECs, providing a source of NO, may undergo an autocrine regulation by NO itself. In fact, NO released by ECs may act directly or after activation of guanylate cyclase on EC membrane pore proteins, thus exerting a powerful effect on EC blood-brain barrier properties, in addition to its well-characterized effects on the adjacent vascular smooth muscle cells. Similarly, cAMP-dependent mechanisms are likely candidates linking EC receptor activation by exogenous transmitters or hormones (resulting in adenylate cyclase activation) to changes in transport properties of the blood-brain barrier. Finally, we hypothesize that pharmaceutical agents capable of selectively affecting EC intracellular communication systems by generation of second messengers such as cGMP and cAMP may be used in order to "permeabilize" the blood-brain barrier to compounds normally excluded by barrier mechanisms and possibly cotransported into the brain by a sodium-dependent facilitated transport mechanism(s).[37,38]

Acknowledgments

This study was supported by a Howard Hughes Medical Institute Physician Research Fellowship (Dr West), the American Heart Association of Washington 91-WA-531, and National Institutes of Health grants NS-51614, NS-30305, NS-

Downloaded from http://ahajournals.org by on February 24, 2022

21076, and NS-07144. We would like to thank K.A. Stanness and D.L. Tinklepaugh for helping in part of the experiments and M.L. Joseph for the continuous assistance in data analysis and for preparation of the figures. We would also like to thank Dr G. Maccaferri for careful revision of the manuscript.

References

1. Bradbury MW, Stulcova B. Efflux mechanism contributing to the stability of the potassium concentration in cerebrospinal fluid. *J Physiol (Lond).* 1970;208:415-430.
2. Betz AL, Firth JA, Goldstein GW. Polarity of the blood-brain barrier: distribution of enzymes between the luminal and antiluminal membranes of the brain capillary endothelial cell. *Brain Res.* 1980;192:17-28.
3. Harik SI. Blood-brain barrier sodium/potassium pump: modulation by central noradrenergic innervation. *Proc Natl Acad Sci U S A.* 1986;83:4067-4070.
4. Betz AL. Sodium transport in capillaries isolated from rat brain. *J Neurochem.* 1983;41:1158-1164.
5. Vigne P, Champigny G, Marsault R, Barbry P, Frelin C, Ladzunski M. A new type of amiloride-sensitive cationic channel in endothelial cells of brain microvessels. *J Biol Chem.* 1989;264:7663-7668.
6. Murphy VA, Johanson CE. Acidosis, acetazolamide, and amiloride: effects on ^{22}Na transfer across the blood-brain and blood-CSF barriers. *J Neurochem.* 1989;52:1058-1063.
7. Goldstein GW. Relation of potassium transport to oxidative metabolism in isolated brain capillaries. *J Physiol (Lond).* 1979;286: 185-195.
8. Ignarro LG. Biological actions and properties of endothelium-derived nitric oxide formed and released from artery and vein. *Circ Res.* 1989;65:1-21.
9. Moncada S, Palmer RMJ, Higgs EA. Nitric oxide: physiology, pathophysiology and pharmacology. *Pharmacol Rev.* 1991;43: 109-142.
10. Prado R, Watson BD, Kuluz J, Dietrich WD. Endothelium-derived nitric oxide synthase inhibition: effects on cerebral blood flow, pial artery diameter, and vascular morphology in rats. *Stroke.* 1992;23: 1118-1123.
11. Kubes P. Nitric oxide modulates epithelial permeability in the feline small intestine. *Am J Physiol.* 1992;262:G1138-G1142.
12. Kubes P. Ischemia-reperfusion in feline small intestine: a role for nitric oxide. *Am J Physiol.* 1993;264:G143-G149.
13. Yuan Y, Granger HJ, Zawieja DC, Chilian WM. Flow modulates coronary venular permeability by a nitric oxide-related mechanism. *Am J Physiol.* 1992;263:H641-H646.
14. Rubin LL, Hall DE, Porter S, Barbu K, Cannon C, Horner HC, Janatpour N, Liaw CW, Manning K, Morales J, Tanner LI, Tommaselli KJ, Bard F. A cell culture model of the blood-brain barrier. *J Cell Biol.* 1991;115:1725-1735.
15. Takeda K, Schini V, Stoeckel H. Voltage-activated potassium but not calcium currents in cultured bovine aortic endothelial cells. *Pflugers Arch.* 1987;410:385-393
16. Hoyer J, Popp R, Meyer J, Galla HJ, Goegelein H. Angiotensin II, vasopressin and GTP-γ-S inhibit inward rectifying K^+ channels in porcine cerebral capillary cells. *J Membr Biol.* 1991;123:55-62.
17. Adams DJ, Barakeh J, Laskey R, Van Breemen C. Ion channels and regulation of intracellular calcium in vascular endothelial cells. *FASEB J.* 1989;3:2389-2400.
18. von der Weid P-I, Beny J-L. Simultaneous oscillations in the membrane potential of pig coronary artery endothelial and smooth muscle cells. *J Physiol (Lond).* 1993;471:13-24.
19. Janigro D, West GA, Gordon EL, Winn HR. ATP-sensitive potassium channels in rat aorta and brain microvascular endothelial cells. *Am J Physiol.* 1993;265:C812-C821.
20. Hammil OP, Marty A, Neher A, Sakmann B, Sigworth FJ. Improved patch-clamp techniques for high-resolution current recording from cells and cell-free membrane patches. *Pflugers Arch.* 1981;391:85-100.
21. Gordon EL, Danielsson PE, Nguyen T-S, Winn HR. A comparison of primary cultures of rat cerebral microvascular endothelial cells to rat aortic endothelial cells. *In Vitro Cell Dev Biol.* 1991;27A: 312-326.
22. Estacion M. Characterization of ion channels seen in subconfluent human dermal fibroblasts. *J Physiol (Lond).* 1991;436:579-671.
23. Maccaferri G, Mangoni M, Lazzari A, DiFrancesco D. Properties of the hyperpolarization-activated current in rat hippocampal pyramidal cells. *J Neurophysiol.* 1993;69:2129-2136.
24. Inoue M, Imanaga G. G protein-mediated inhibition of inwardly rectifying K^+ channels in guinea pig chromaffin cells. *Am J Physiol.* 1993;265:C946-C956.
25. DiFrancesco D, Ferroni A, Mazzanti M, Tromba C. Properties of the hyperpolarizing-activated current (i_f) in cells isolated from the sino-atrial node. *J Physiol (Lond).* 1986;377:61-88.
26. DiFrancesco D. Characterization of single pacemaker channels in cardiac sino-atrial node cells. *Nature.* 1986;324:470-473.
27. DiFrancesco D. The cardiac hyperpolarizing-activated current i_f: origins and developments. *Prog Biophys Mol Biol.* 1985;46:163-183.
28. McCormick DA, Pape HC. Properties of a hyperpolarization-activated cation current and its role in rhythmic oscillation in thalamic relay neurons. *J Physiol (Lond).* 1990;431:291-318.
29. McCormick DA, Pape HC. Noradrenergic and serotonergic modulation of a hyperpolarization-activated cation current in thalamic relay neurons. *J Physiol (Lond).* 1990;431:319-342.
30. Schwindt PC, Spain WJ, Crill WE. Influence of anomalous rectifier activation on afterhyperpolarizations of neurons from cat sensorimotor cortex in vitro. *J Neurophysiol.* 1988;59:468-481.
31. Pape HC, Mager R. Nitric oxide controls oscillatory activity in thalamocortical neurons. *Neuron.* 1992;9:441-448.
32. Brown AM, Birnbaumer L. Direct G protein gating of ion channels. *Am J Physiol.* 1988;254:H401-H410.
33. DiFrancesco D. Block and activation of the pace-maker channel in calf Purkinje fibres: effects of potassium, caesium and rubidium. *J Physiol (Lond).* 1982;329:485-507.
34. Clapp LH, Gurney AM. Modulation of calcium movements by nitroprusside in isolated vascular smooth muscle cells. *Pflugers Arch.* 1991;418:462-470.
35. DiFrancesco D, Tortora P. Direct activation of cardiac pacemaker channels by intracellular cyclic AMP. *Nature.* 1991;351:145-147.
36. Feelisch M, Noack EA. Correlation between nitric oxide formation during degradation of organic nitrates and activation of guanylate cyclase. *Eur J Pharmacol.* 1987;139:19-30.
37. Watanabe H, Kuhne W, Schwartz P, Piper M. A2-adenosine receptor stimulation increases macromolecule permeability of coronary endothelial cells. *Am J Physiol.* 1992;262:H1174-H1181.
38. Balestrino M, West GA, Winn HR, Janigro D. Blockade of inward potassium currents by GTP-γ-S in endothelial cells. Soc. for Neuroscience Annual Meeting; 1993; Washington, DC.
39. Colden-Standfield M, Cramer EB, Gallin EK. Comparison of apical and basal surfaces of confluent endothelial cells: patch-clamp and viral studies. *Am J Physiol.* 1992;263:C573-C583.
40. Ho WK, Brown HF, Noble D. Internal K ions modulate the action of external cations on hyperpolarizing-activated inward current in rabbit isolated sinoatrial node cells. *Pflugers Arch.* 1993;424: 308-314.
41. Buga GM, Griscavage JM, Rogers NE, Ignarro LJ. Negative feed-back regulation of endothelial cell function by nitric oxide. *Circ Res.* 1993;73:808-812.
42. Filep JG, Földes-Filep E, Sirois P. Nitric oxide modulates vascular permeability in the rat coronary circulation. *Br J Pharmacol.* 1993; 108:323-326.
43. Olesen S-P. Regulation of ion permeability in frog brain venules: significance of calcium, cyclic nucleotides and protein kinase C. *J Physiol (Lond).* 1987;387:59-68.
44. Lansman JB, Hallam TJ, Rink TJ. Single stretch-activated ion channels in vascular endothelial cells as mechanotransducers? *Nature.* 1987;325:611-613.

Downloaded from http://ahajournals.org by on February 24, 2022